Air Emissions Due to Wind and Solar Power

Warren Katzenstein and Jay Apt

Supporting Information

1. Regression Analyses

Data

Each emissions data set contains six variables: date, time, power generated, heat rate, NO_x mass emission, and a calibration flag. We model only NO_x and CO_2 emissions from the turbine. Carbon monoxide is emitted and is regulated for natural gas turbines but we do not consider CO in the present analysis.

CO_2 Approach

The LM6000 data (fig. S1 and S2) were divided into four regions corresponding to startup, ramping up to full power, full power, and ramping down to shutdown phases (identified as regions 1, 2, 3, and 4, respectively in fig. S3).

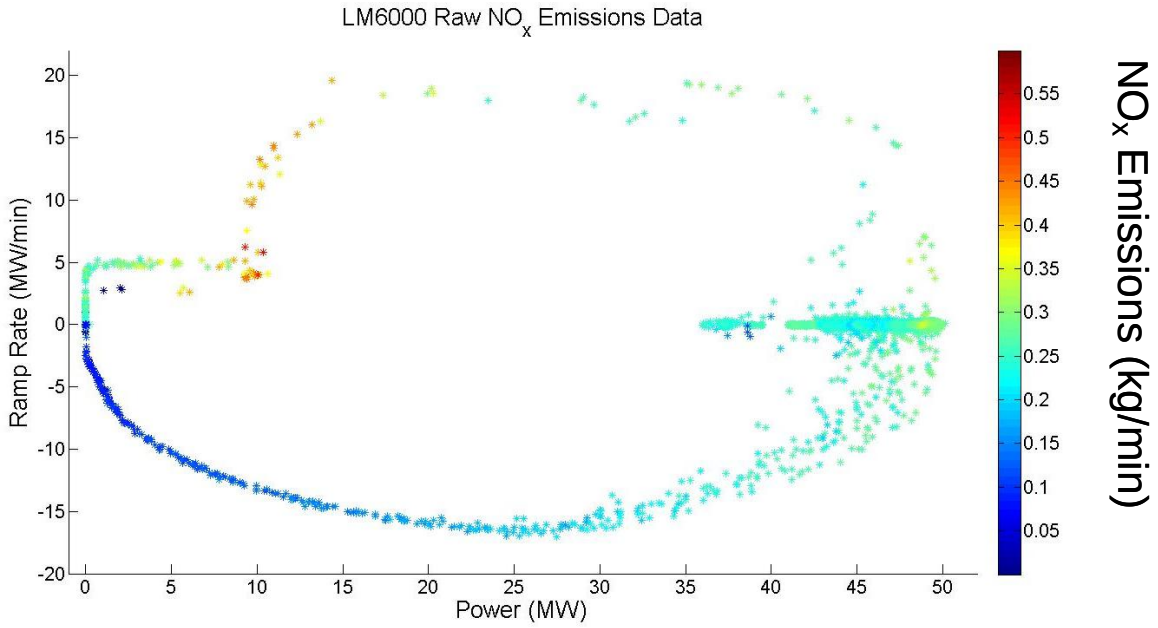

Figure S1 - LM6000 raw NO_x emissions data.

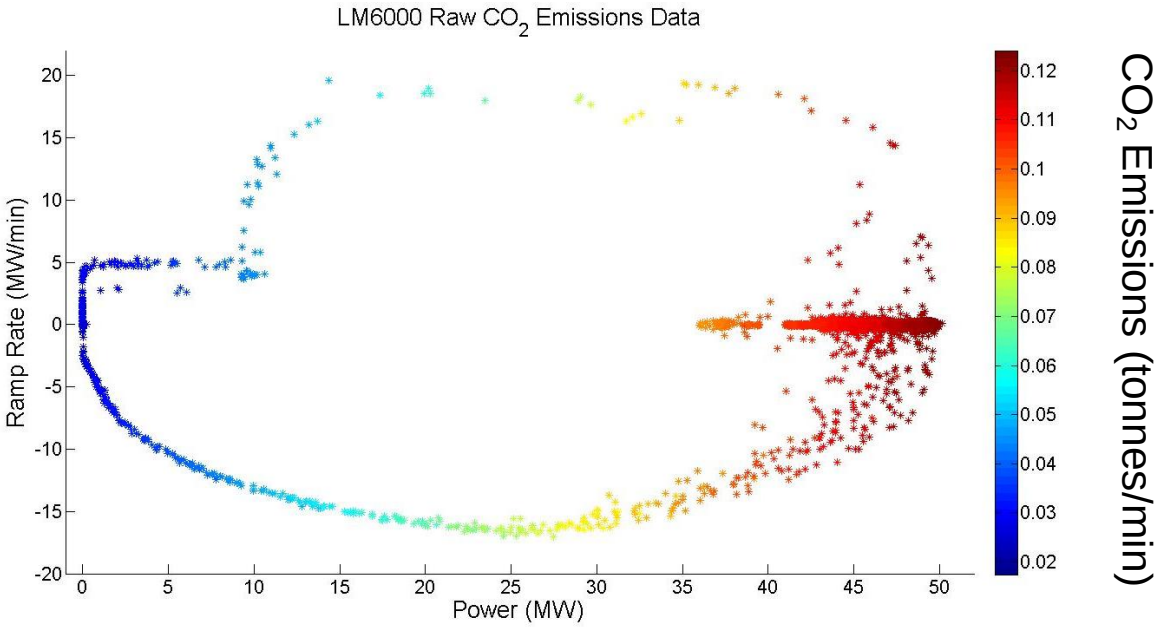

Figure S2 - LM6000 raw CO_2 emissions data.

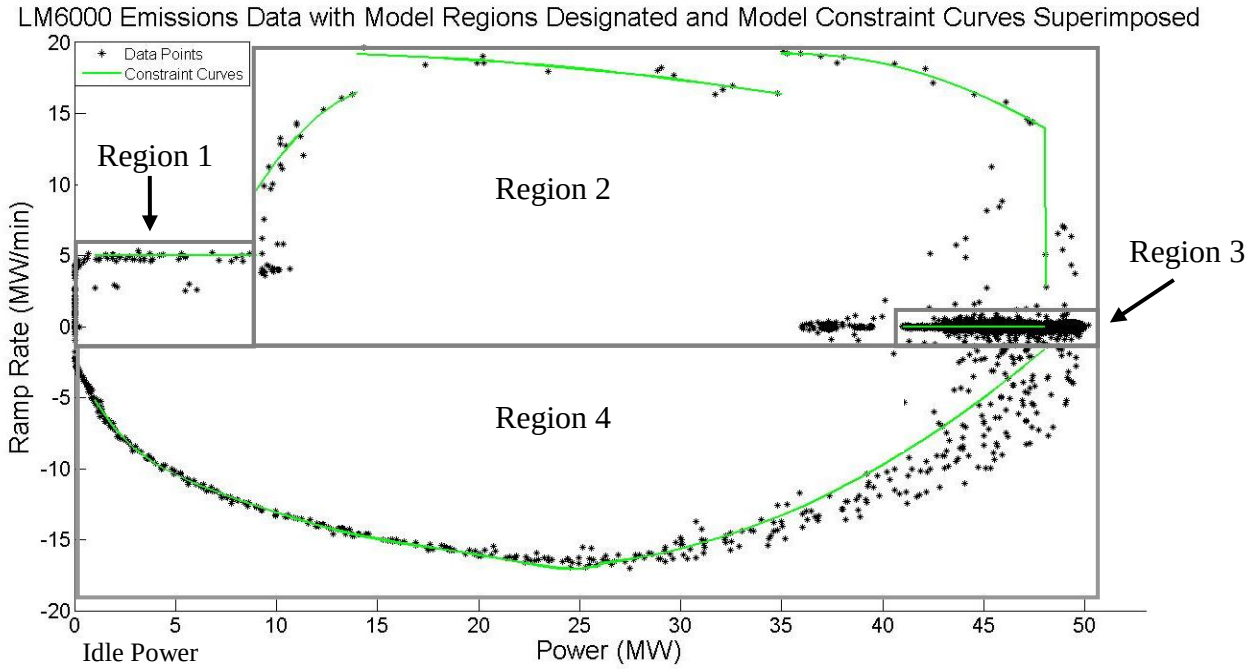

Figure S3 - LM6000 emissions data. The emissions data were divided into four regions which were modeled independently. The constraint curves imposed by the populated data are shown for each region.

We performed a multiple regression on each region (equations S1 – S4); the goodness of fit is shown in figures S4 and S5, by graphing the absolute percent error between a regression model and the corresponding NO_x emissions data. The 501FD CO_2 data were not divided into multiple regions, as they depend on only the turbine's power level; a linear regression analysis was performed (equation S5 and Figure S6). Adjusted R^2 values are in Table S1 and detailed statistical information on the regression analyses can be found in Tables S2 and S3.

LM6000 CO_2 Regression Results (in tonnes / min)

Region 1 $$\frac{dM_{CO2,LM6000}}{dt} = 2.68x10^{-2} + 1.77x10^{-3} P_{LM6000} \quad \text{(S1)}$$

Region 2 $$\frac{dM_{CO2,LM6000}}{dt} = 3.18x10^{-2} - 1.54x10^{-3} P_{LM6000} + 5.82x10^{-6} P_{LM6000}^2 - 2.54x10^{-4} \dot{P}_{LM6000} \quad \text{(S2)}$$

Region 3 $$\frac{dM_{CO2,LM6000}}{dt} = 3.6x10^{-1} + 1.26x10^{-3} P_{LM6000} + 9.27x10^{-6} P_{LM6000}^2 \quad \text{(S3)}$$

Region 4 $$\frac{dM_{CO2,LM6000}}{dt} = 2.72x10^{-2} + 1.88x10^{-3} P_{LM6000} - 9.207x10^{-6} \dot{P}_{LM6000} \quad \text{(S4)}$$

501FD CO_2 Regression Results (in tonnes / min)

Region 1 $$\frac{dM_{CO2,501FD}}{dt} = 1.18x10^{-1} + 1.84x10^{-3} P_{LM6000} \quad \text{(S5)}$$

TABLE S1 – Adjusted R^2 values for the regressions used to model each region of each turbine and pollutant.

Adjusted R^2 Values				
Region	**1**	**2**	**3**	**4**
LM6000				
CO_2	0.85	0.99	0.86	0.99
NO_x	0.85	0.84	-	0.94
501FD				
CO_2	0.99	-	-	-
NO_x	0.72	0.64	0.28	-

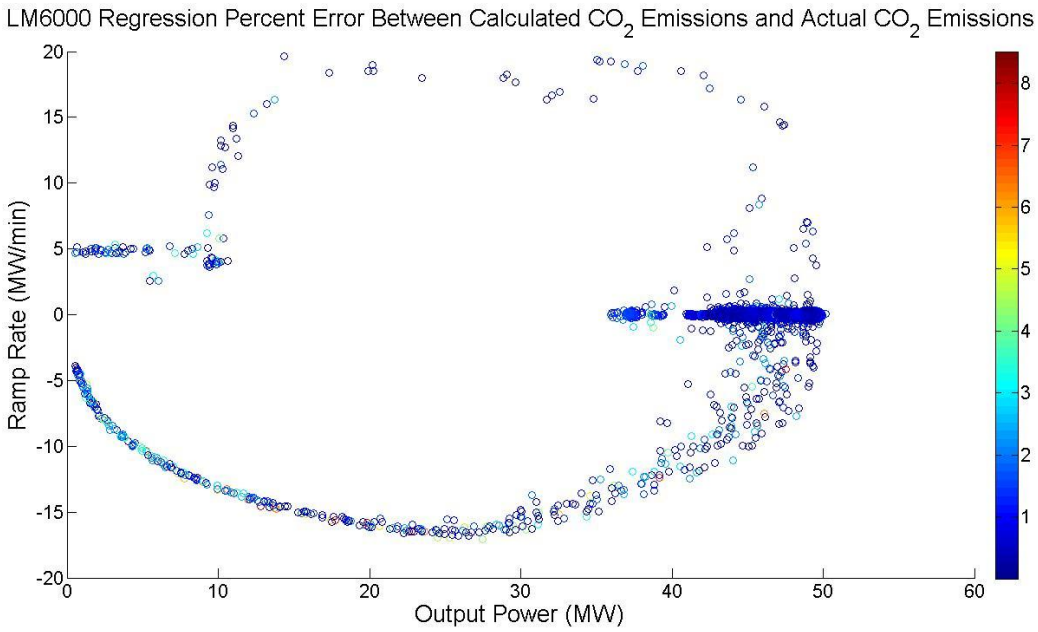

Figure S4 – Absolute percent error between calculated CO_2 emissions based on regressions and actual CO_2 emissions from LM6000 data set.

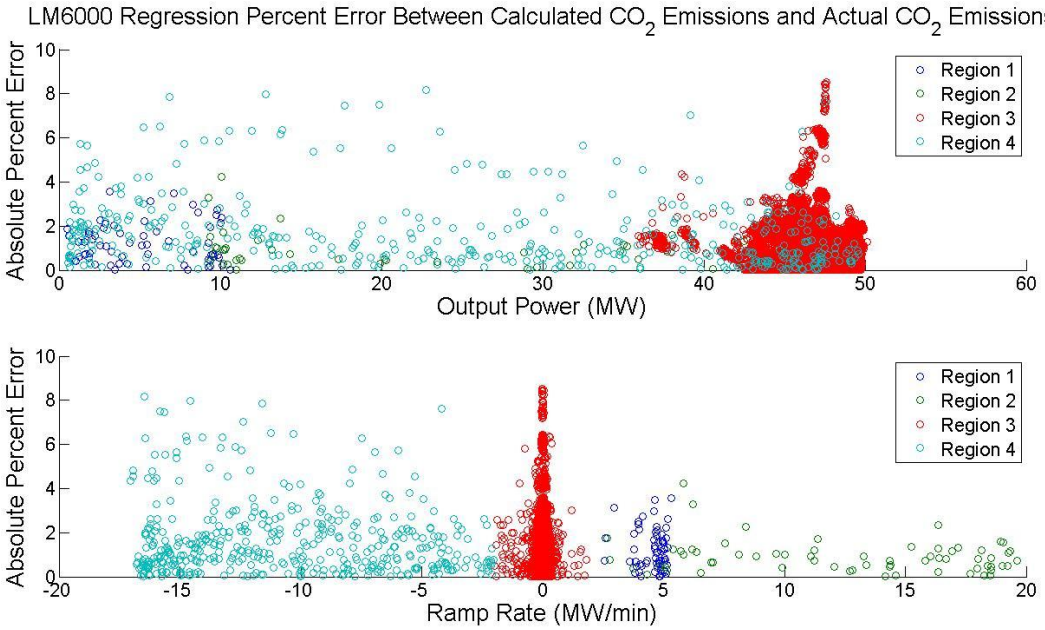

Figure S5 – Absolute percent error between calculated CO_2 emissions based on regressions and actual CO_2 emissions from LM6000 data set. Results are colored according to the regions (fig. S3). Top: absolute percent error for each data point versus power level. Bottom: absolute percent error for each data point versus ramp rate.

Table S2 - LM6000 Region CO_2 Regression Results

Region 1

Equation $$\frac{dM_{CO2,LM\,6000}}{dt} = 2.68x10^{-2} + 1.77x10^{-3} P_{LM\,6000} \quad [tonnes/\min]$$

Regression Statistics

Adjusted R^2	0.85
# of Data Points	134
F-value	731.81
Prob>F	<0.0001
Root MSE	$2.63x10^{-3}$

Parameter Statistics

Intercept	Std. Error	$2.84x10^{-4}$		
	t-value	4.34	Prob > |t|	<0.0001
$P_{LM\,6000}$	Std. Error	$6.54x10^{-5}$		
	t-value	27.05	Prob > |t|	<0.0001

Region 2

Equation $$\frac{dM_{CO2,LM\,6000}}{dt} = 3.18x10^{-2} - 1.54x10^{-3} P_{LM\,6000} + 5.82x10^{-6} P_{LM\,6000}^2 - 2.54x10^{-4} \dot{P}_{LM\,6000} \quad [tonnes/\min]$$

Regression Statistics

Adjusted R^2	0.999
# of Data Points	65
F-value	21,893.8
Prob>F	<0.0001
Root MSE	$9.22x10^{-4}$

Parameter Statistics

Intercept	Std. Error	$5.53x10^{-4}$		
	t-value	57.54	Prob > |t|	<0.0001
$P_{LM\,6000}$	Std. Error	$7.29x10^{-5}$		
	t-value	21.15	Prob > |t|	<0.0001
$P_{LM\,6000}^2$	Std. Error	$1.3x10^{-6}$		
	t-value	4.48	Prob > |t|	<0.0001
$R_{LM\,6000}$	Std. Error	$3.44x10^{-5}$		
	t-value	-7.38	Prob > |t|	<0.0001

Region 3

Equation $$\frac{dM_{CO2,LM\,6000}}{dt} = 3.6x10^{-1} + 1.26x10^{-3} P_{LM\,6000} + 9.27x10^{-6} P_{LM\,6000}^2 \quad [tonnes/\min]$$

Regression Statistics

Adjusted R^2	0.864
# of Data Points	15,845
F-value	50,487.5
Prob>F	<0.0001
Root MSE	$1.64x10^{-3}$

Parameter Statistics

Intercept	Std. Error	$3.6x10^{-3}$		
	t-value	9.99	Prob > |t|	<0.0001
$P_{LM\,6000}$	Std. Error	$1.58x10^{-4}$		
	t-value	8.03	Prob > |t|	<0.0001
$P_{LM\,6000}^2$	Std. Error	$1.72x10^{-6}$		
	t-value	5.39	Prob > |t|	<0.0001

Region 4

Equation $$\frac{dM_{CO2,LM\,6000}}{dt} = 2.72x10^{-2} + 1.88x10^{-3} P_{LM\,6000} - 9.207x10^{-6} \dot{P}_{LM\,6000} \quad [tonnes/\min]$$

Regression Statistics

Adjusted R^2	0.998
# of Data Points	447
F-value	88,330.9
Prob>F	<0.0001
Root MSE	$1.62x10^{-3}$

Parameter Statistics

Intercept	Std. Error	$2.72x10^{-2}$		
	t-value	122.72	Prob > |t|	<0.0001
$P_{LM\,6000}$	Std. Error	$4.48x10^{-6}$		
	t-value	420.07	Prob > |t|	<0.0001
$P_{LM\,6000}^2$	Std. Error	$1.66x10^{-5}$		
	t-value	-5.52	Prob > |t|	<0.0001

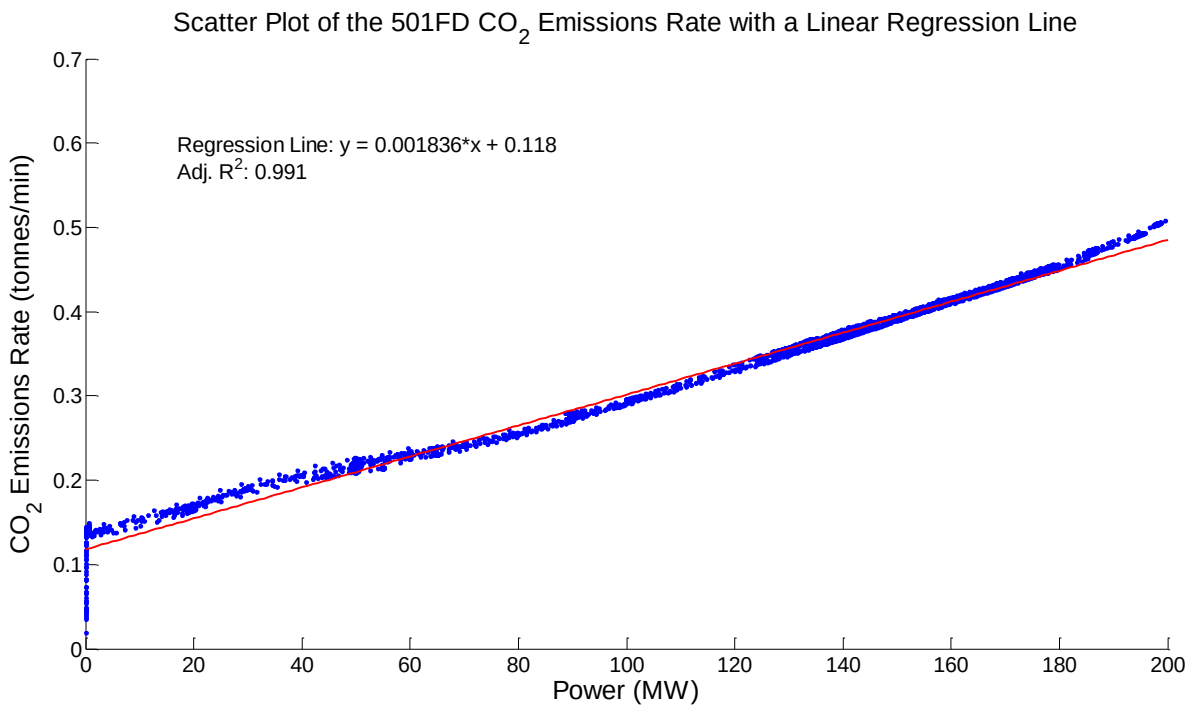

Figure S6 - CO_2 emissions rate for the 501FD turbines as a function of turbine output power (blue dots) and the linear regression model used to characterize the CO_2 emissions rate (red line). The linear regression equation is y = 0.00184x + 0.118 and has an adjusted R^2 value of 0.991.

Table S3 - 501FD Region CO_2 Regression Analysis Results

Region 1

Equation $$\frac{dM_{CO2,501FD}}{dt} = 1.18x10^{-1} + 1.84x10^{-3} P_{LM\,6000} \quad [tonnes/\min]$$

Regression Statistics

Adjusted R^2	0.991
# of Data Points	6,501
F-value	711,368
Prob>F	<0.0001
Root MSE	$7.29x10^{-3}$

Parameter Statistics

Intercept	Std. Error	$2.88x10^{-4}$		
	t-value	416.07	Prob > |t|	<0.0001
P_{501FD}	Std. Error	$2.16x10^{-6}$		
	t-value	843.43	Prob > |t|	<0.0001

NO_x Approach

Available NO_x combustion control technologies are water (liquid or steam) injection systems and dry low-NO_x combustion designs [1]. The LM6000 data were obtained from 45 MW turbines that injected steam into the combustion chambers, lowering flame temperatures to reduce NO_x. The 200 MW 501FD turbines used General Electric's Dry-Low NO_x (DLN) system of lean premixed combustion. The median nameplate size for all US natural gas turbines using Dry Low NO_x control is 170 MW; using steam injection it is 80 MW. Thus, the turbines for which we have data are moderately representative.

In GE's Dry-Low NO_x systems, fuel is premixed with air to create a fuel-lean mixture that is burned in a two-stage process to reduce flame temperatures and residence times. At full generator output, GE's DLN operates at a mixture just richer than the flame blowout point of natural gas. As the generator load is reduced, less fuel is fed to the combustion chamber resulting in lower flame temperatures. As load is reduced further the flame blowout point is reached and GE's DLN system can no longer employ the fuel-lean premixed firing mode, and shifts to a diffusion flame where high flame temperatures are present. As a result, low NO_x emission rates are achieved in the power range of approximately 50% to 100% of nameplate capacity and NO_x emission rates an order of magnitude greater are observed in the power range of 0% to 50% [2].

Taking the same approach used to model CO_2 emissions, we modeled NO_x emission rates as a function of power level and ramp rate (equations S6 – S9). For region 3, no satisfactory result could be derived and the mean of the data was used (standard deviation of 0.022). Figures S8 and S9 display the goodness of fit for each regression.

The 501FD NO_x data were divided into three regions: low power, medium power, and full power (labeled regions 1, 2, and 3, respectively). Equations S10 – S12 are the regression results for the 501FD data and figure S7 compares the regression results with the 501FD NO_x

emission data. Adjusted R^2 values can be found in Table S1 and detailed statistical information can be found in Tables S4 and S5.

LM6000 NO_x Regression Results (in kg / min)

Region 1
$$\frac{dM_{NOx,LM\,6000}}{dt} = 1.31x10^{-1} + 6.62x10^{-2} P_{LM\,6000} - 3.89x10^{-3} \dot{P}_{LM\,6000} \quad \text{(S6)}$$

Region 2
$$\frac{dM_{NOx,LM\,6000}}{dt} = 6.76x10^{-1} - 2.27x10^{-2} P_{LM\,6000} + 3.27x10^{-4} P^2_{LM\,6000} - 1.3x10^{-2} \dot{P}_{LM\,6000} + 6.53x10^{-4} \dot{P}^2_{LM\,6000} \quad \text{(S7)}$$

Region 3
$$\frac{dM_{NOx,LM\,6000}}{dt} = 2.68x10^{-1} \quad \text{(S8)}$$

Region 4
$$\frac{dM_{NOx,LM\,6000}}{dt} = 8.35x10^{-2} + 7.53x10^{-4} P_{LM\,6000} - 3.85x10^{-3} P^2_{LM\,6000} \quad \text{(S9)}$$

501FD NO_x Regression Results (in kg / min)

Region 1
$$\frac{dM_{NOx,501FD}}{dt} = 8.03x10^{-1} + 2.45x10^{-2} P_{501FD} - 3.49x10^{-4} P^2_{501FD} \quad \text{(S10)}$$

Region 2
$$\frac{dM_{NOx,501FD}}{dt} = -9.48x10^{-1} + 6.12x10^{-2} P_{501FD} - 3.95x10^{-4} P^2_{501FD} \quad \text{(S11)}$$

Region 3
$$\frac{dM_{NOx,501FD}}{dt} = 1.18x10^{-1} - 5.76x10^{-4} P_{501FD} + 4.1x10^{-6} P^2_{501FD} \quad \text{(S12)}$$

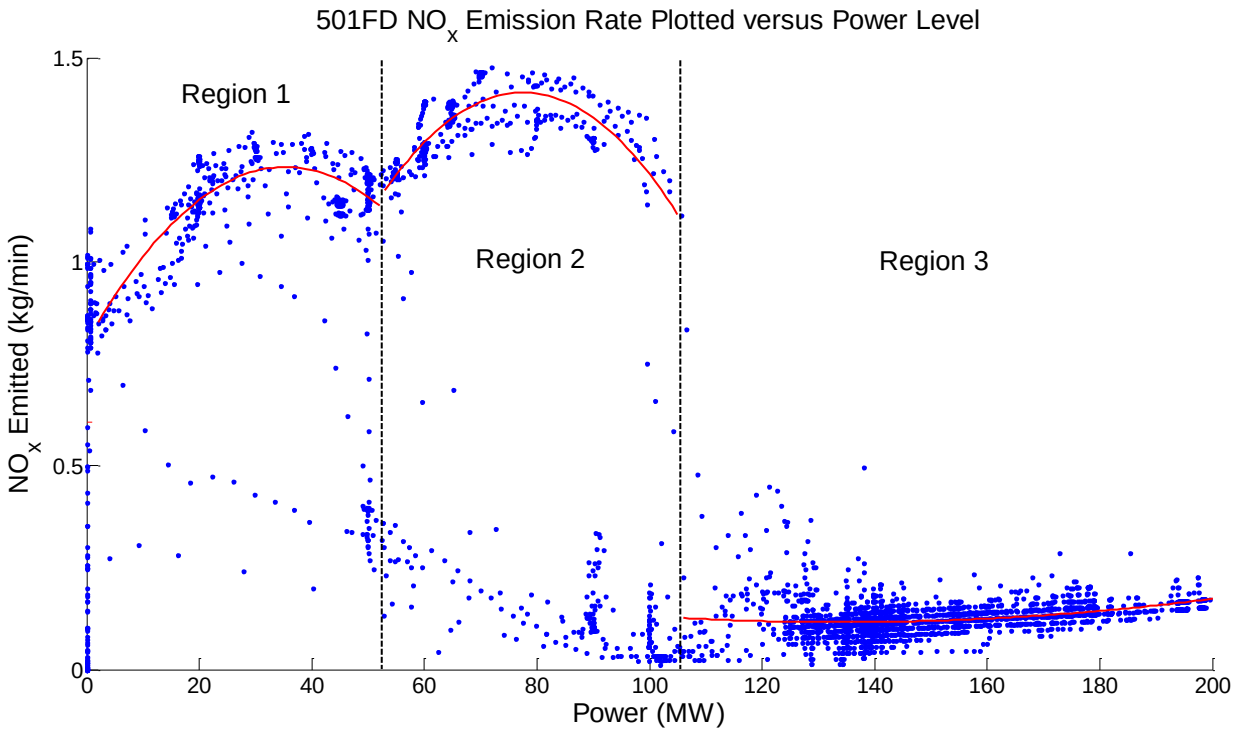

Figure S7 - 501FD NOx emissions data as a function of power (blue dots) and regression (red line). The emissions data were divided into three regions which were modeled independently of each other. This combined-cycle turbine is designed to produce low NOx only when operated at high power.

Table S4 - 501FD Region NO_x Regression Results

Region 1

Equation $$\frac{dM_{NOx,501FD}}{dt} = 8.03x10^{-1} + 2.45x10^{-2} P_{501FD} - 3.49x10^{-4} P_{501FD}^2 \quad [kg/\min]$$

Regression Statistics

Adjusted R^2	0.72
# of Data Points	463
F-value	723.12
Prob>F	<0.0001
Root MSE	$6.99x10^{-2}$

Parameter Statistics

Intercept	Std. Error	$6.99x10^{-3}$		
	t-value	124.45	Prob > |t|	<0.0001
P_{501FD}	Std. Error	$6.44x10^{-4}$		
	t-value	30.03	Prob > |t|	<0.0001
P_{501FD}^2	Std. Error	$1.18x10^{-5}$		
	t-value	-23.13	Prob > |t|	<0.0001

Region 2

Equation $$\frac{dM_{NOx,501FD}}{dt} = -9.48x10^{-1} + 6.12x10^{-2} P_{501FD} - 3.95x10^{-4} P_{501FD}^2 \quad [kg/\min]$$

Regression Statistics

Adjusted R^2	0.64
# of Data Points	562
F-value	489
Prob>F	<0.0001
Root MSE	$4.58x10^{-2}$

Parameter Statistics

Intercept	Std. Error	$7.26x10^{-2}$		
	t-value	-12.98	Prob > |t|	<0.0001
P_{501FD}	Std. Error	$2.0x10^{-3}$		
	t-value	30.47	Prob > |t|	<0.0001
P_{501FD}^2	Std. Error	$1.33x10^{-5}$		
	t-value	-29.49	Prob > |t|	<0.0001

Region 3

Equation $$\frac{dM_{NOx,501FD}}{dt} = 1.18x10^{-1} - 5.76x10^{-4} P_{501FD} + 4.1x10^{-6} P_{501FD}^2 \quad [kg/\min]$$

Regression Statistics

Adjusted R^2	0.28
# of Data Points	5,129
F-value	979.37
Prob>F	<0.0001
Root MSE	$1.02x10^{-2}$

Parameter Statistics

Intercept	Std. Error	$1.96x10^{-2}$		
	t-value	6.10	Prob > |t|	<0.0001
P_{501FD}	Std. Error	$2.52x10^{-4}$		
	t-value	-2.39	Prob > |t|	<0.0001
P_{501FD}^2	Std. Error	$7.98x10^{-7}$		
	t-value	5.24	Prob > |t|	0.0002

LM6000 Regression Analysis

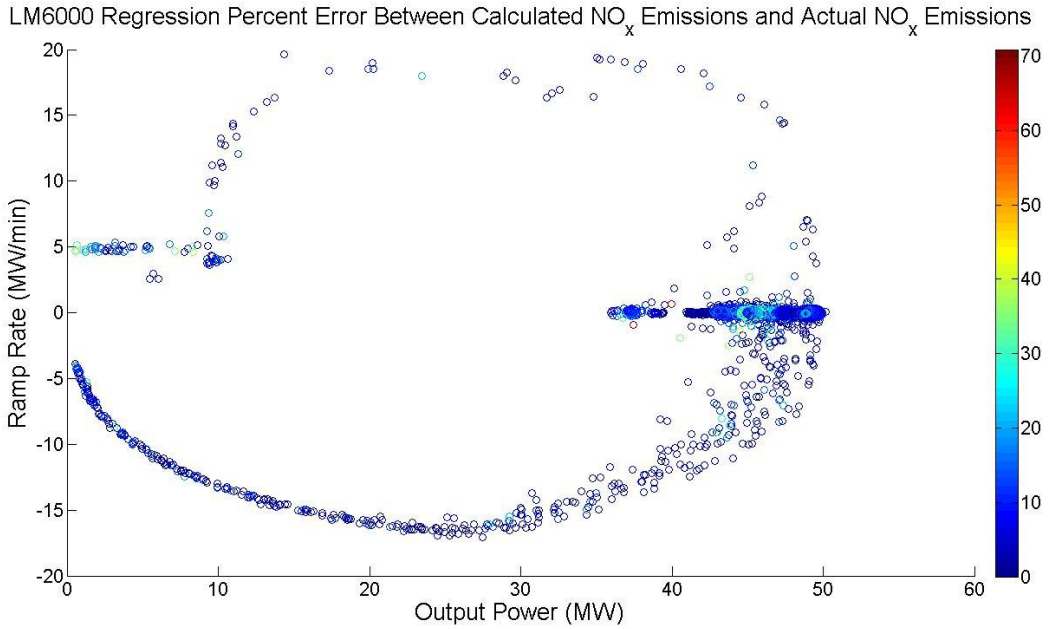

Figure S8 - Absolute percent error between calculated NO_x emissions based on regressions and actual NO_x emissions from LM6000 data set.

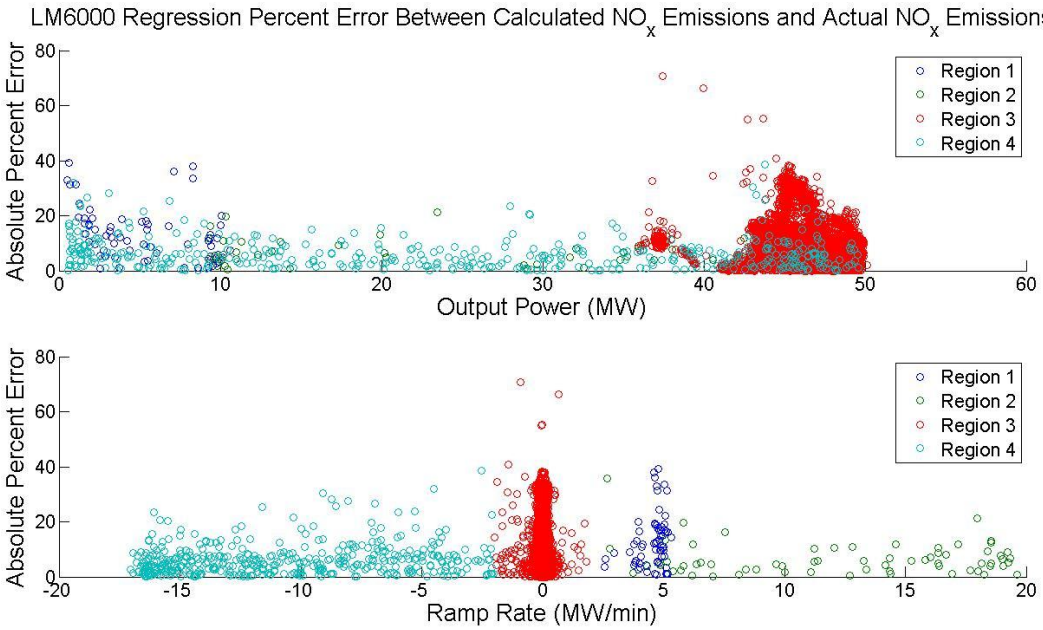

Figure S9 - Absolute percent error between calculated NO_x emissions based on regressions and actual NO_x emissions from LM6000 data set. Results are colored according to the regions (fig. S3). Top: absolute percent error for each data point versus power level. Bottom: absolute percent error for each data point versus ramp rate.

Table S5 - LM6000 Region NO_x Regression Results

Region 1

Equation $$\frac{dM_{NOx,LM\,6000}}{dt} = 1.31x10^{-1} + 6.62x10^{-2} P_{LM\,6000} - 3.89x10^{-3} \dot{P}_{LM\,6000} \quad [kg/\min]$$

Regression Statistics

Adjusted R^2	0.85
# of Data Points	134
F-value	159.56
Prob>F	<0.0001
Root MSE	$5.26x10^{-2}$

Parameter Statistics

Intercept	Std. Error	$6.99x10^{-3}$		
	t-value	13.64	Prob > |t|	<0.0001
$P_{LM\,6000}$	Std. Error	$1.6x10^{-3}$		
	t-value	11.77	Prob > |t|	<0.0001
$R_{LM\,6000}$	Std. Error	$2.48x10^{-3}$		
	t-value	13.18	Prob > |t|	<0.0001

Region 2

Equation $$\frac{dM_{NOx,LM\,6000}}{dt} = 6.76x10^{-1} - 2.27x10^{-2} P_{LM\,6000} + 3.27x10^{-4} P_{LM\,6000}^2 - 1.3x10^{-2} \dot{P}_{LM\,6000} + 6.53x10^{-4} \dot{P}_{LM\,6000}^2 \quad [kg/\min]$$

Regression Statistics

Adjusted R^2	0.84
# of Data Points	65
F-value	83.56
Prob>F	<0.0001
Root MSE	$2.95x10^{-2}$

Parameter Statistics

Intercept	Std. Error	$3.96x10^{-2}$		
	t-value	17.13	Prob > |t|	<0.0001
$P_{LM\,6000}$	Std. Error	2.74x10-3		
	t-value	-8.27	Prob > |t|	<0.0001
$P_{LM\,6000}^2$	Std. Error	$4.81x10^{-5}$		
	t-value	6.83	Prob > |t|	<0.0001
$R_{LM\,6000}$	Std. Error	$4.85x10^{-3}$		
	t-value	-2.69	Prob > |t|	0.0094
$R_{LM\,6000}^2$	Std. Error	$2.18x10^{-4}$		
	t-value	2.99	Prob > |t|	0.004

Region 3

Equation $$\frac{dM_{NOx,LM\,6000}}{dt} = 2.68x10^{-1} \quad [kg/\min]$$

Mean Statistics

Standard Deviation	0.0222	# of Data Points	15,844

Region 4

Equation $$\frac{dM_{NOx,LM\,6000}}{dt} = 8.35x10^{-2} + 7.53x10^{-4} P_{LM\,6000} - 3.85x10^{-3} P_{LM\,6000}^2 \quad [kg/\min]$$

Regression Statistics

Adjusted R^2	0.94
# of Data Points	447
F-value	3,486
Prob>F	<0.0001
Root MSE	$1.67x10^{-2}$

Parameter Statistics

Intercept	Std. Error	$1.72x10^{-3}$		
	t-value	50.2	Prob > |t|	<0.0001
$P_{LM\,6000}$	Std. Error	1.91e-4		
	t-value	23.7	Prob > |t|	<0.0001
$P_{LM\,6000}^2$	Std. Error	3.89e-6		
	t-value	-3.71	Prob > |t|	0.0002

2. Regressions Constraints

LM6000 Regression Constraints

The LM6000 turbines were generally operated in a consistent manner (figs. S1-S3): initialized, ramped up quickly and held at or near full power, and ramped quickly down, and turned off. Thus, not all the power-ramp-rate control space is sampled in the data we obtained. We applied constraints to our LM6000 model to ensure the model turbine was operated in regions sampled by the actual data (green lines in fig. S3).

Compensating for wind or solar power fluctuations in the simulations required some power and ramp rate combinations not situated on a constraint curve; we created an ensemble of samples from points on the constraint curves to match the desired combinations. We found that in doing so, the maximum error in the base load plant's output was 7.6% and the mean error was 1.6%. It is possible that our approach produces inaccurate results due to the incompletely sampled power-ramp-rate control space.

501FD Regression Constraints

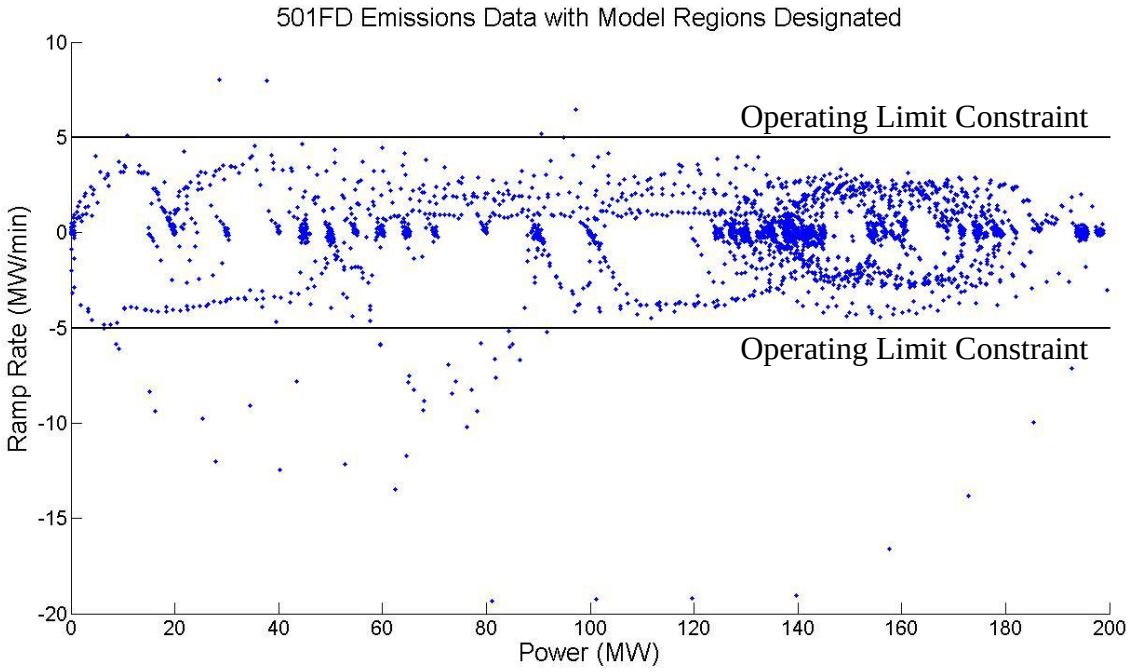

Figure S10 - 501FD emissions data. The boundaries on the model's ramp rate, imposed by the populated data points in the control map, are shown. The 501FD was operated in a manner that sampled more points in its control map than the LM6000 and as a result the 501FD model is not as constrained as the LM6000 model.

The 501FD was cycled through its control space in a manner that sampled more points (fig. S10) than the LM6000 turbines. As a result, the 501FD model is not as strictly constrained as the LM6000 model. The only constraints imposed on the 501FD model were limitations on the maximum and minimum ramp rates, set at 5 MW/min and -5 MW/min, respectively.

3. Profile Sensitivity Analysis Raw Data

The results of the model are dependent upon how much the gas turbine(s) ramp through their power range and at what power levels they are required to operate. Therefore, the results seen in Table 1 of the main paper, obtained from using the full time series of the 5 data sets (see Table S6), estimates only the emission reductions for the conditions that existed during the periods when the data were collected. Ideally, a significant number of high time-resolution independent

power plant outputs would be used in our simulations. However we did not have access to such a data set, only to the 5 data sets described.

TABLE S6. Wind and solar photovoltaic data sets from utility-scale sites used in the analysis. The maximum observed power of several of the power plants exceeded their nameplate capacity; in other cases the nameplate capacity was not reached during the period for which data were obtained.

Data set	Power plant type	Capacity factor based on nameplate wind or PV size	Normalized capacity factor based on maximum observed power	Resolution	Data set length
Eastern	Wind	0.07	0.12	1 second	240 hours
Northern Great Plains	Wind	0.57	0.59	10 second	15 hours
Central Great Plains	Wind	0.53	0.54	10 second	84 hours
Southern Great Plains	Wind	0.50	0.46	10 second	370 hours
Southwest	Solar PV	0.19	0.19	1 minute	732 days

For wind data, one could imagine generating theoretical wind data, subject to certain constraints, such as ensuring the appropriate frequency and phase characteristics [3, 4]. Instead, we relied on the actual high time resolution data, creating smaller data subsets from the initial data thereby creating a large collection of data sets that represent a variety of variable power plant outputs. To create the smaller data sets, a sliding window 1,000 minutes in length was used to produce smaller data samples 1,000 minutes long. The Eastern wind plant data, recorded over a 10 day period, is 14,400 minutes in length and using the sliding window produced 13,401 data subsets. Each data subset differs from the preceding data subset by two data points. Therefore, there is a significant amount of correlation between the smaller data sets and it is this correlation that produces the lines, or tracks, seen in Figures S11 through S14.

For the solar PV data, each day that power was produced was used as a data subset. The solar data obtained was 732 days in length and thus produced 732 data subsets used in the profile sensitivity analysis.

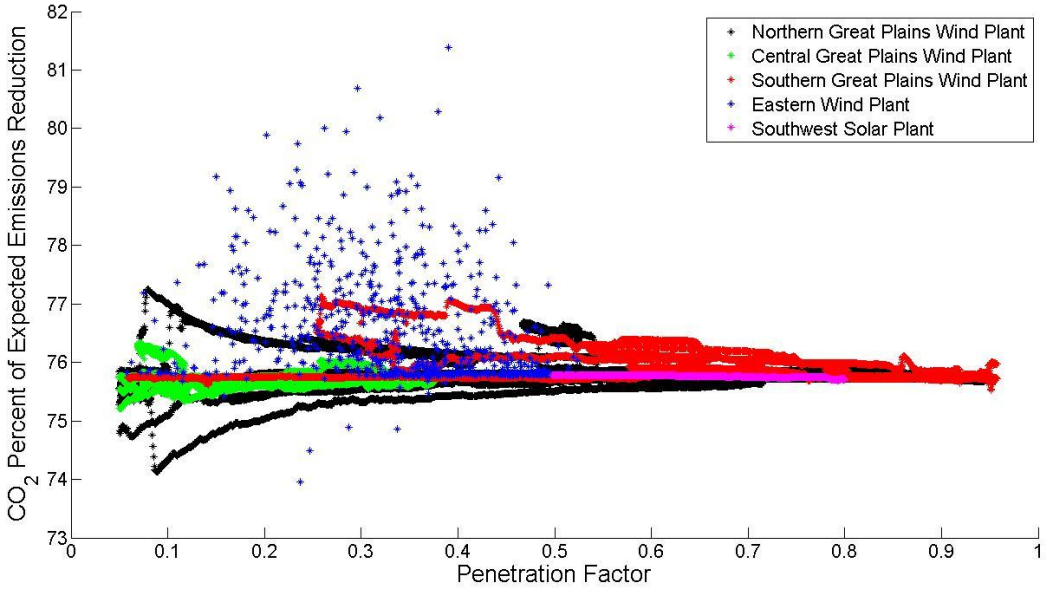

Figure S11 - 501FD CO_2 expected emissions reduction raw results from profile sensitivity analysis.

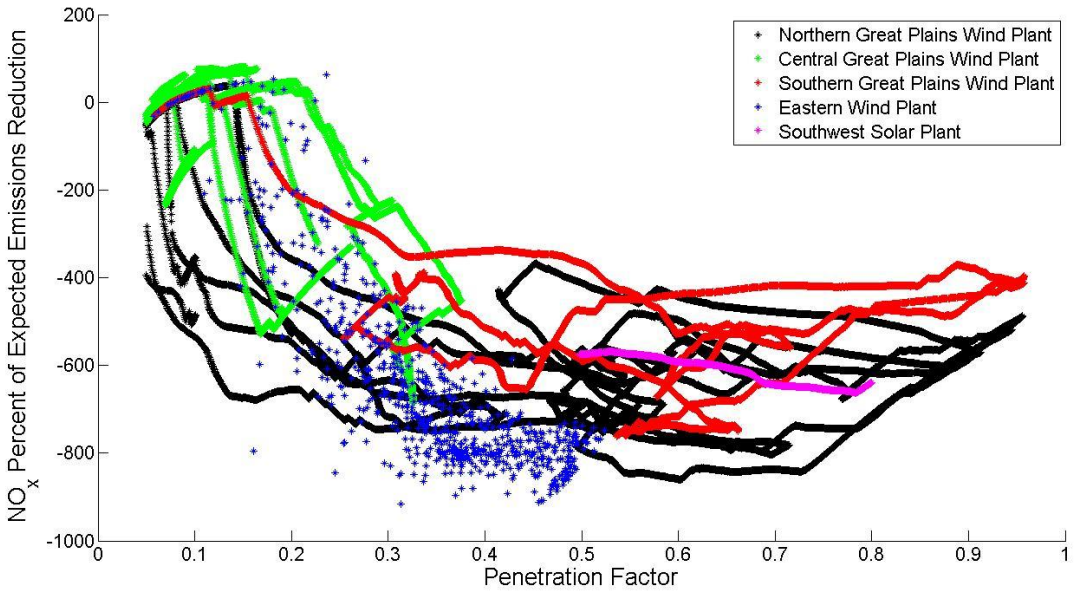

Figure S12 - 501FD NO_x expected emissions reduction raw results from profile penetration analysis.

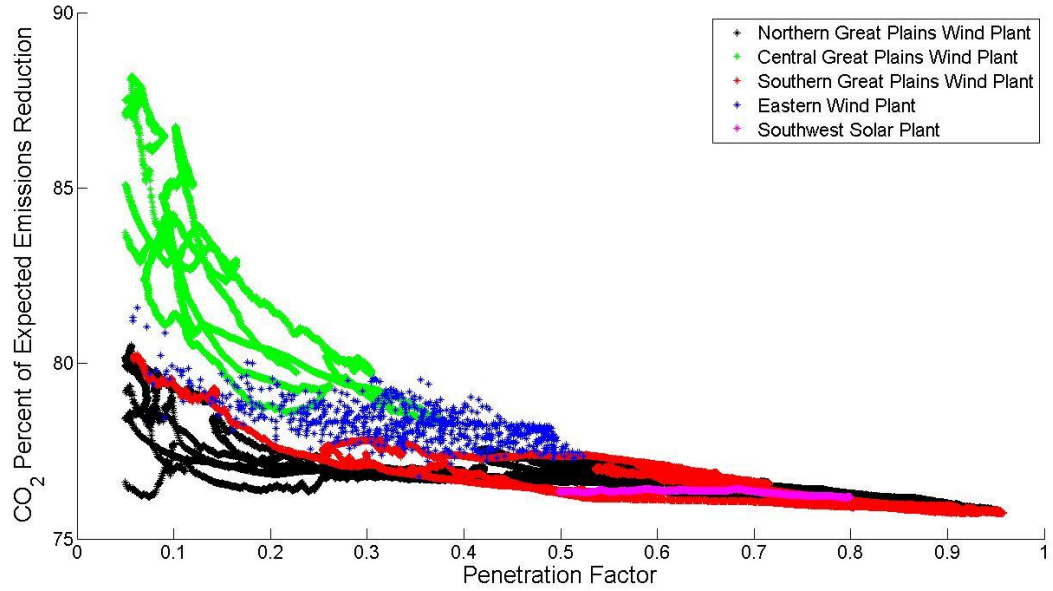

Figure S13 - LM6000 CO_2 expected emissions reduction raw results from profile penetration analysis.

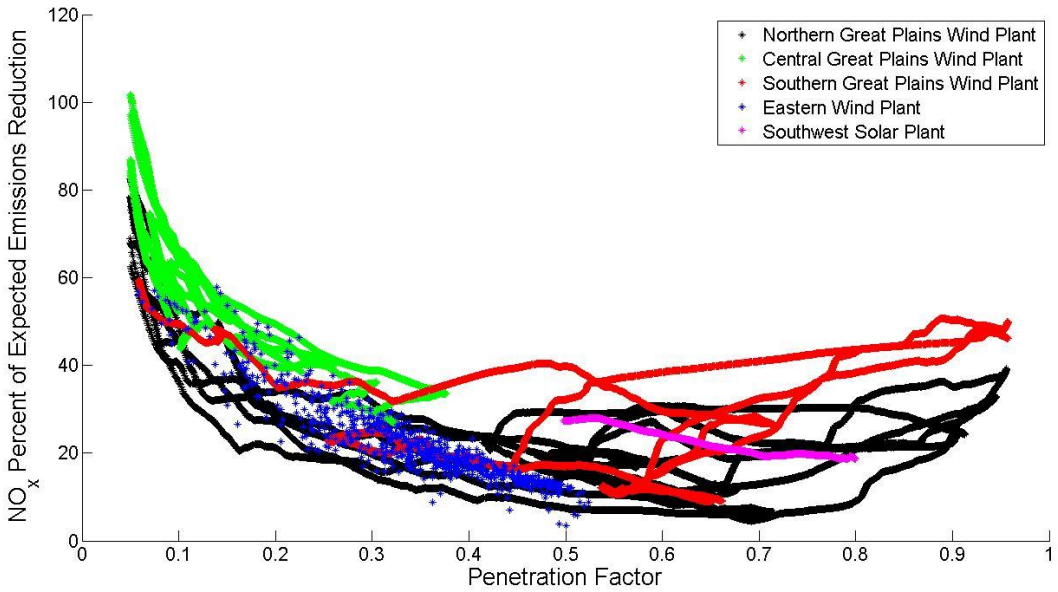

Figure S14 - LM6000 NO_x expected emissions reduction raw results from profile penetration analysis.

4. Multiple Turbine Analysis

In order to investigate how emissions are affected by the penetration factor of wind, the constraint of pairing the wind farm with only one natural-gas turbine is relaxed. One to five natural-gas turbines were paired with the wind farm to produce a base load variable plant of size $n \cdot P$ MW, where n is the number of turbines and P is the power limit of the turbine. The fill-in power required is divided equally among the turbines and as a result the lower power limit of the turbines is P - P/n MW.

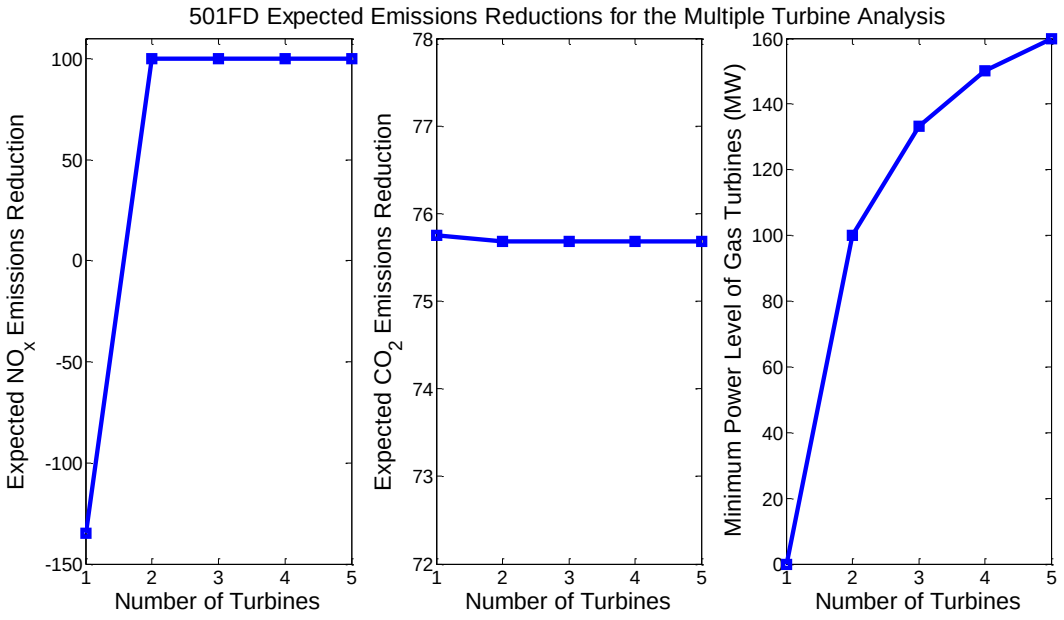

Figure S15 - 501FD multiple turbine analysis using the Eastern wind data set. By pairing *n* 501FD turbines with a variable power plant, the lower power limit (P_{min}) of the turbines is P - P/*n* MW. For 2 or more turbines, P_{min} is greater than 50% of the 501FD's nameplate capacity and NO_x emissions are reduced according to expectations. If no attention is paid to P_{min}, NO_x emissions increase.

Figure S15 shows the results of the multiple turbine analysis for 501FD turbines using the Eastern wind data set. Limiting the minimum operating power level of the natural-gas turbine in the variable base load plant produces significantly better NO_x emissions performance. By limiting a 501FD to power regions of 50% of nameplate capacity or greater, the poor emissions

performance region of GE's DLN system, where NO_x emissions are an order of magnitude higher, is avoided and emissions are displaced at effectively a linear rate and match expectations. Limiting the minimum power level has no effect upon the CO_2 emissions performance when using 501FDs.

5. Literature Cited

[1] U.S. Environmental Protection Agency. *Alternative Control Techniques Document – NO_x Emissions from Stationary Gas Turbines*; EPA-453/R-93-007; Emission Standards Division: Washington, DC, 1993. http://www.epa.gov/ttn/catc/dir1/gasturb.pdf

[2] Davis, L.B.; Black, S.H. Dry Low NO_x Combustion Systems for GE Heavy-Duty Gas Turbines; GER-3568G; General Electric Power Systems: Schenectady, NY, 2000. http://www.gepower.com/prod_serv/products/tech_docs/en/downloads/ger3568g.pdf

[3] Apt, J. The Spectrum of Power from Wind Turbines. *J. of Power Sources*. **2007**, 169 (2), 369-374.

[4] Curtright, A.; Apt, J. The Character of Power Output from Utility-Scale Photovoltaic Systems. *Progress in Photovoltaics*. **2008**. 16 (3), 241-247.